



ELSEVIER

Contents lists available at ScienceDirect

## Polymer Testing

journal homepage: [www.elsevier.com/locate/polytest](http://www.elsevier.com/locate/polytest)POLYMER  
TESTING

ROGER BROWN

## Material Characterisation

# Characterization of HDPE-g-MA/clay nanocomposites prepared by different preparation procedures: Effect of the filler dimension on crystallization, microhardness and flammability

Liliya Minkova<sup>a,\*</sup>, Sara Filippi<sup>b</sup><sup>a</sup> Institute of Polymers, Bulgarian Academy of Sciences, Sofia 1113, Bulgaria<sup>b</sup> Department of Chemical Engineering, University of Pisa, 56126 Pisa, Italy

## ARTICLE INFO

## Article history:

Received 2 September 2010

Accepted 13 October 2010

## Keywords:

HDPE-g-MA/organoclay nanocomposites

Preparation procedures

Crystallization

Microhardness

Flammability

## ABSTRACT

Nanocomposites of maleic anhydride-grafted HDPE (HDMA) and the organoclay Cloisite 20A (20A) have been prepared by melt-compounding, solution-blending and static annealing of polymer/clay powder mixtures. It has been shown that solution-blending of HDMA with 20A fails to produce intercalated composites. Fast intercalation was observed when solution-blending HDMA/clay composites were annealed. The nanocomposites prepared in the melt under shear were found to possess high levels of exfoliation.

The dependence of the crystallization behaviour, microhardness and flammability of the composites on the preparation conditions has been studied by differential scanning calorimetry, microhardness tests and determination of limiting oxygen index. The results have shown that the reduction of the flammability and the microhardness of HDMA/20A nanocomposites prepared by melt compounding and composite annealing are higher than those for composites prepared by solution blending. Moreover, a nucleation effect of the clay on the polymer matrix crystallization for some samples has been observed. The results have been interpreted by different levels of clay dispersion and degree of clay intercalation/exfoliation, achieved during different preparation procedures.

© 2010 Elsevier Ltd. All rights reserved.

## 1. Introduction

On practical grounds, solution-blending is certainly a nanocomposite preparation procedure of lesser importance, compared to melt-compounding, as it involves usage of environmentally unfriendly solvents. However, from a scientific point of view, a comparison of the structure and morphology of polymer/clay composites obtained by different procedures, solution-blending inclusive, is extremely useful. That allows clarifying the relative importance of the different parameters which influence the intercalation and exfoliation processes, such as stress involved in melt-compounding, temperature, polymer-

organoclay compatibility, etc. It has been shown that significant levels of intercalation or exfoliation are achieved for linear low density polyethylene or polypropylene nanocomposites prepared from solution without compatibilizers [1,2]. However, only microcomposites are known to be produced from the same components by melt-compounding [3,4]. A comparison of the structures and morphologies of poly(ethylene-co-acrylic acid)/organoclay composites prepared from solution or by annealing in the melt, with or without shear, has been published [5]. Although a wide range of solvents was employed in the solution-blending preparations, only unintercalated microcomposites were obtained by this procedure, regardless of whether solvent was removed by evaporation or by precipitation in different non-solvents. On the contrary, extremely fast intercalation was monitored when the precipitated microcomposites, or even mechanical mixtures of the powdered components, were

\* Corresponding author. Tel.: +359 2 9793668.

E-mail address: [lminkova@gmx.net](mailto:lminkova@gmx.net) (L. Minkova).

melted or annealed at temperatures close to the melting point [5].

In a previous paper [6], one of us has reported on the structure and morphology of nanocomposites of maleic anhydride-grafted high density polyethylene (HDMA) and the organoclay Cloisite 20A (20A). It has been shown that solution-blending of HDMA with 20A fails to produce intercalated composites. Fast intercalation was observed when solution-blending HDMA/clay composites were annealed. The nanocomposites prepared in the melt under shear were found to possess high levels of exfoliation [6].

The present work reports on the dependence of the crystallization behavior, microhardness and flammability of the HDMA/clay composites on the preparation conditions studied by differential scanning calorimetry, microhardness tests and determination of limiting oxygen index.

## 2. Experimental

### 2.1. Materials

The polymers used in this work were: Polybond<sup>®</sup> 3009 (HDMA), a HDPE grafted with MA (1 wt%) with MFI = 5 dg min<sup>-1</sup>, kindly provided by Chemtura, and Eltex<sup>®</sup> B5920 (HDPE) with MFI = 0.39 dg min<sup>-1</sup> and  $d = 950 \text{ kg m}^{-3}$ , provided by Solvay. The commercial organoclay, Cloisite<sup>®</sup> 20A (20A), was supplied by Southern Clay Products, Inc.

In this paper, the investigated composites are indicated by the matrix symbol (HDPE or HDMA) followed by a figure corresponding to the inorganic MMT content in phr.

### 2.2. Preparation of the composites from solution

A weighed amount of the polymer (about 5 g) was first dissolved under stirring in hot xylene (about 200 mL). The appropriate volume of a dispersion of the organoclay in the same solvent (2 wt%), prepared by stirring and gentle heating for 2 h, was then added to the polymer solution. The stirring was continued for 2 h. A portion of the solution was placed in an aluminum pan and evaporated at room temperature, first at atmospheric pressure for 1–7 days and then under vacuum for at least two days. The remaining hot solution was poured into excess acetone under vigorous stirring and the precipitated fine powder was separated on a sintered glass filter, washed several times with fresh acetone and dried under vacuum at room temperature. Different solvents, such as toluene and 1,2,4-trichlorobenzene, and different non-solvents, such as ethyl alcohol, pentane and THF, were employed occasionally for comparison.

### 2.3. Preparation of the composites by melt-compounding

The polymer pellets and the clay were dried in a vacuum oven at 60 °C overnight and were fed to a Brabender Plasticorder static mixer of 50 mL capacity, preheated to 150 °C. The rotor speed was maintained at 30 rpm for about 3 min and was then increased gradually (in 30 s) to 60 rpm. During the mixing time (10 min), the temperature rose by 10–15 K, due to stress heating. The molten composites were extracted from the mixer and cooled naturally in air.

### 2.4. Preparation of the composites by quiescent annealing

The powder obtained by precipitation from solution as described above was compressed at room temperature to prepare 2 mm thick tablets of 20 mm in diameter. Similar tablets were prepared from mechanical mixtures of powdered polymer and clay. The tablets were then placed in a mold consisting of a 2 mm thick stainless steel plate with a hole of 20 mm in diameter, sandwiched between two steel plates covered with anti-adherent film. The mold was heated at the selected temperature for different times in a Carver press before being cooled naturally or quenched with ice-water.

### 2.5. Study of the crystallization behavior of the composites prepared with different procedures

Calorimetric measurements were made on a Perkin Elmer DSC-7 instrument, calibrated with indium and tin standards, under a nitrogen atmosphere. The specimens were heated to 190 °C and kept at this temperature for 5 min in order to destroy the polyethylene crystal nuclei. The DSC cooling traces were recorded at rates of 1, 5 and 10 °C/min. The degree of crystallinity was calculated from the crystallization enthalpy, normalized to the polymer content. The enthalpy of crystallization of 100% crystalline functionalized polyethylene was taken as 293.1 J/g. For accurate determination of the non-isothermal kinetic characteristics, the apparatus was calibrated at various scanning rates. The lag between sample and pan holder temperatures was estimated according to the procedure of Eder and Wlochowicz [7]. The Harnisch and Muschik equation was used for the determination of the Avrami exponents [8].

DSC experiments of isothermal crystallization were carried out as follows: the specimens were heated to 190 °C at a rate of 10 °C/min, kept at this temperature for 5 min and cooled to the appropriate crystallization temperature  $T_c$  (in the 120–124 °C range) at a rate of 200 °C/min. The heat evolved during isothermal crystallization was recorded and the fraction  $X_t$  of the polymer crystallized at time  $t$  was evaluated as the ratio of the area under the curve at time  $t$  to that of the whole exotherm. The starting time of crystallization was taken as that at which thermal equilibrium was reached at  $T_c$ . The area of the exotherm was measured by back extrapolation of the baseline after complete crystallization.

### 2.6. Microhardness measurements of the composites prepared with different procedures

The specimens used for the measurement of microhardness were compression molded disks of 8 mm diameter and 1 mm thickness. Microhardness of the materials was measured on a standard Vickers microhardness tester mhp-160 with a light microscope NU-2 (Germany).

The indenter was a square shaped diamond pyramid with top angle of 136°. Loads of 0.4, 0.6, 0.8 and 1.0 N to correct the instant elastic recovery were employed. A loading cycle of 0.5 min was used. The standard Vickers microhardness ( $H$ ) was determined by the equation [9,10]:

$$H = K \frac{P}{d^2} \quad (1)$$

where  $P$  is the applied load,  $k$  is a geometric factor equal to 1.854 and  $d$  is the mean diagonal length of the imprint, measured after removing the indenter. At least 10 imprints were made for each load. The  $H$  value was determined within  $\Delta H/H = 0.05$ . Under the loads applied, the mean diagonal length of the imprints varied in the range 100–200  $\mu\text{m}$ .

### 2.7. Determination of the flammability of the composites prepared with different procedures

The flammability of neat polymers and composites was evaluated by determining their limiting oxygen index (LOI). The specimens for the measurements were compression molded plates with length of 40 mm, width of 10 mm and thickness of 2 mm, prepared by hot pressing of the materials at 190 °C. The determination of LOI of the samples was performed using a FTA flammability apparatus supplied by Stanton Redcroft.

## 3. Results and discussion

It has been shown that solution-blending of HDPE or HDMA with 20A fails to produce intercalated composites, as long as solvent removal is made at room temperature (Fig. 1 A) [6]. Although the organoclay is predominantly exfoliated when dispersed in a good solvent of the polymer, such as hot xylene, it tends to reaggregate when the solvent is removed. Evaporation or precipitation in non-solvents led to homogeneous dispersion of (fairly small) unintercalated tactoids in the polymer matrix. On the contrary, fast intercalation is observed when polymer/clay blends are annealed, with no shear, at temperatures higher than the melting point of the polymer (Fig. 1B) [6]. When applied to HDMA/clay blends prepared from solution, this thermal treatment does even lead to fully exfoliated or disorderly intercalated nanocomposites. Finally, nanocomposites prepared in the melt under shear have been found to possess high levels of exfoliation, at least for clay loadings up to about 15 wt%. (Fig. 1C) [6].

### 3.1. Crystallization behavior of the nanocomposites

The crystallization of HDMA and of chosen nanocomposites prepared by solution blending or by melt blending has been studied by isothermal DSC analysis in the range of crystallization temperatures between 120 and 124 °C. It should be stated that the clay remains in the solid state over the whole temperature interval covered during the measurements. Thus, the recorded isothermal DSC traces consist of single exothermic peaks. The isothermal crystallization parameters are collected in Table 1. It is apparent that the addition of the clay into HDMA for melt blending samples does not change significantly, or slightly increases, the half-crystallization times of the polymer (Table 1). On the contrary, for solution blending samples, the addition of the clay into HDMA decreases the half-crystallization times of the polymer (Table 1). In order to

analyze more precisely the influence of the addition of the clay on the overall crystallization rate of the matrix polymer the isothermal crystallization kinetics have been studied.

The isothermal crystallization kinetics has been analyzed by the Avrami equation:

$$X_t = 1 - \exp(-Kn.t^n) \quad (2)$$

where  $X_t$  is the fraction crystallized at time  $t$ ,  $KN$  the kinetic constant and  $n$  the Avrami exponent depending on the nucleation type and the growth geometry of the crystals. Values of  $Kn$  and  $n$  can be obtained from the intercepts and slopes, respectively, of the linear plots of  $\log(-\ln(1-X_t))$  vs.  $\log t$ . Examples of these plots for HDMA and a nanocomposite, prepared by solution blending (HDMA-6.2 sol) are shown in Fig. 2a,b. The Avrami exponents for HDMA and the nanocomposites are in the range 2.5–3.0, indicating athermal nucleation and three-dimensional growth. The results show that the addition of the clay does not change the isothermal crystallization mechanism of the matrix phase. The values of the kinetic constants for HDMA and the nanocomposites are also collected in Table 1. As seen, the values of these constants for nanocomposites prepared by solution blending are higher than that measured for neat HDMA. These results confirm that the nanoclay has a nucleating role for the polyethylenes matrix crystallization in solution blended composites. On the contrary, in melt blended composites, the values of kinetic constants do not change significantly in comparison to those of neat HDMA.

The crystallization of HDMA and chosen nanocomposites, prepared by solution blending, melt blending and static annealing has been investigated under non-isothermal conditions using different cooling rates, as described in the experimental section. The dependence of the crystallization temperature on the clay concentration at a cooling rate of 10 °C/min is shown on Fig. 3. Obviously, the crystallization temperature of solution blended samples is higher than that of neat HDMA, while the crystallization temperature of melt blended samples and samples prepared by static annealing does not change significantly in comparison to that of neat HDMA. The overall non-isothermal crystallization kinetics of HDMA, without and in the presence of clay, has been studied by the Harnisch and Muschik method. The Avrami exponents  $n$  have been determined according to the following equation, which is valid at  $T = T_c$ :

$$n = 1 + \frac{\{\ln[y_1/(1-x_1)] - \ln[y_2/(1-x_2)]\}}{\ln(f_2/f_1)} \quad (3)$$

where  $x_i$  is the crystalline fraction calculated by integration of the DSC endotherm;  $y_i$  is the derivative of  $x_i$  and  $f_i$  is the cooling rate used in the experiment. The Avrami exponents  $n$  for HDMA and its nanocomposites have been measured from the plots of  $\ln[y/(1-x)]$  vs.  $T$ . An example for such a plot is shown in Fig. 4 for HDMA-6.2 composite prepared by solution blending. The values of Avrami exponents for all samples are in the range 2.8–3.1, indicating athermal nucleation and three-dimensional growth. The results show that the addition of clay to HDMA does not change the non-isothermal crystallization mechanism of the matrix phase. This result is in accordance with the isothermal measurements.

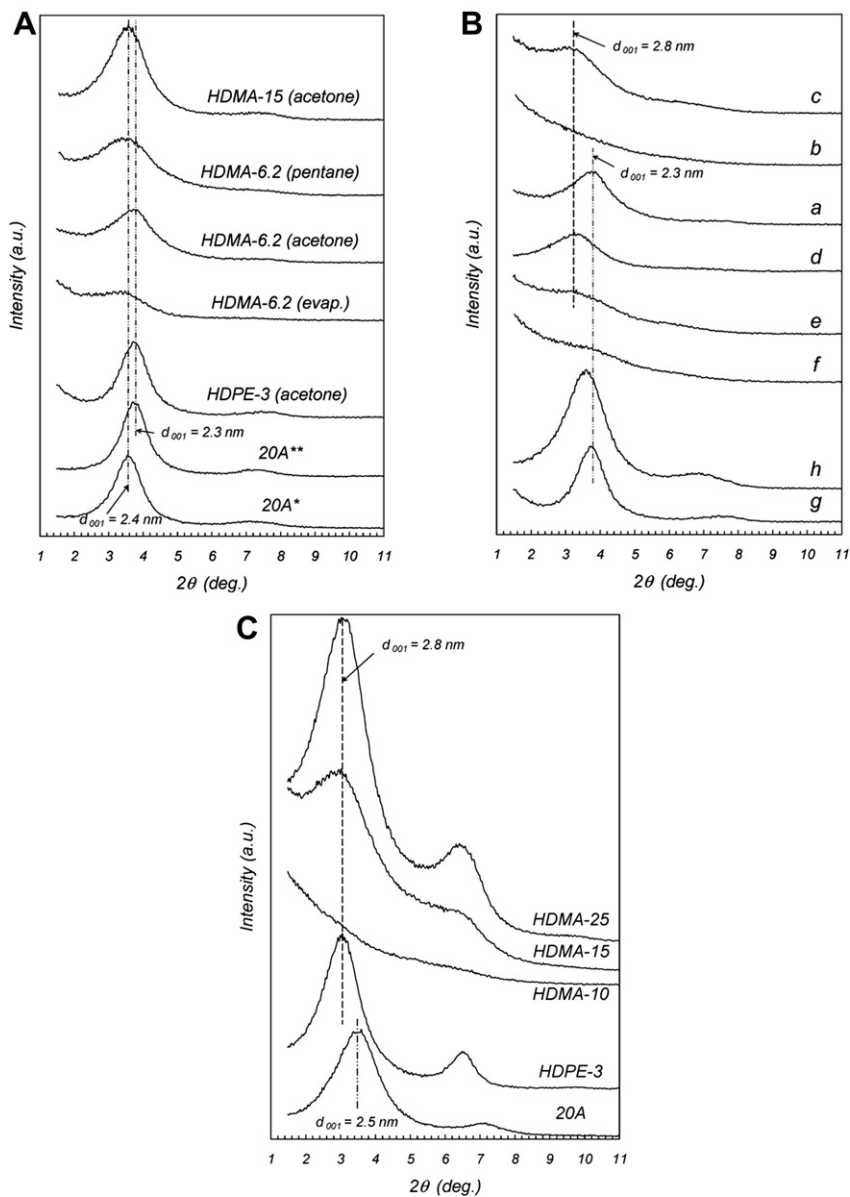


**Fig. 1.** (A) XRD patterns of the 20A\* and 20A\*\* clays (respectively prepared by precipitation in excess ethanol or acetone of a 20A xylene dispersion) and of tablets of the powders obtained from xylene solutions of polymer and clay by precipitation in the indicated non-solvents, or by solvent evaporation, dried under vacuum at room-temperature; (B) Effect of the thermal treatments on the XRD patterns of some HDMA and HDPE composites prepared from solution in hot xylene and precipitation in acetone. (a) HDMA-6.2, no treatment; (b) HDMA-6.2, melted at 190 °C and cooled slowly in the mold; (c) HDMA-15, melted at 190 °C and cooled slowly in the mold; (d) HDMA-6.2, annealed 21 h at 110 °C; (e) HDMA-6.2, held unstirred 1 min at 150 °C and quenched in ice-water; (f) HDMA-6.2, held unstirred 5 min at 150 °C and quenched in ice-water; (g) HDPE-3, no treatment; (h) HDPE-3, melted at 190 °C and cooled slowly in the mold; (C) XRD patterns of the as received 20A and some of the HDPE/20A and HDMA/20A composites prepared by melt-compounding (the figures indicate the clay loading as phr of inorganic material) [6].

The results from the study of the crystallization behavior of HDMA nanocomposites prepared by different procedures lead to the following conclusion: The addition of the clay does not change the HDMA crystallization mechanism under non-isothermal and isothermal conditions. The isothermal overall crystallization rate of HDMA in nanocomposites prepared by melt blending is almost unchanged in comparison to that of neat HDMA. On the other hand, the

overall crystallization rate of HDMA in nanocomposites prepared by solution blending increases due to the increased nucleation rate. These results could be interpreted by the different level of clay dispersion and degree of clay intercalation/exfoliation achieved during different preparation procedures. Evidently, only the unintercalated tactoids of the clay with dimensions of the order of microns in solution blended samples can guarantee sufficient

**Table 1**  
Isothermal crystallization parameters of HDMA and its nanocomposites.

Sample	$T_c$ (°C)	$t_{0.5}$ (s)	$n$	$K_n$ (s <sup>-n</sup> )
HDMA	124	269	2.7	$1.9 \times 10^{-7}$
	123	194	2.7	$4.5 \times 10^{-7}$
	122	140	2.5	$2.9 \times 10^{-6}$
	121	102	2.5	$6.5 \times 10^{-6}$
	120	75	2.5	$1.4 \times 10^{-5}$
HDMA-10 melt	124	302	2.9	$4.4 \times 10^{-8}$
	123	187	2.9	$1.7 \times 10^{-7}$
	122	133	2.8	$7.8 \times 10^{-7}$
	121	95	2.7	$3.1 \times 10^{-6}$
	120	68	2.8	$5.1 \times 10^{-6}$
HDMA-6.2 sol	124	205	3.0	$8.0 \times 10^{-8}$
	123	110	3.0	$5.2 \times 10^{-7}$
	122	95	2.9	$1.2 \times 10^{-6}$
	121	68	2.8	$5.1 \times 10^{-6}$
	120	45	2.7	$2.3 \times 10^{-5}$
HDMA-15 sol	124	175	2.9	$2.1 \times 10^{-7}$
	123	117	2.8	$1.1 \times 10^{-6}$
	122	63	2.8	$6.3 \times 10^{-6}$
	121	53	2.8	$1.0 \times 10^{-5}$
	120	42	2.7	$2.8 \times 10^{-5}$

nucleation density, which increases the polymer matrix crystallization. On the contrary, the nucleation density supplied by exfoliated clay layers in melt blended samples is not enough to provoke the increase in the overall crystallization rate of the matrix polymer. Similar results have been published for melt blended nanocomposites based on low density polyethylene, containing 3 or 6% of nanoclay; the nanocomposites exhibit exfoliated structure and no significant nucleation activity of the clay was observed [11].

### 3.2. Microhardness of the nanocomposites

The experimental hardness values of the neat HDMA and the nanocomposites prepared by different procedures are collected in Table 2. According to the additivity law, the microhardness of materials is determined by the equation:

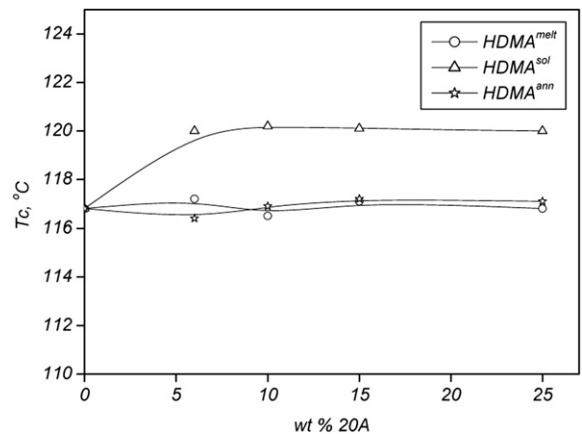


**Fig. 3.** Dependence of crystallization temperature on the clay concentration for HDMA composites, prepared by different procedures.

$$H = w \cdot H^{\text{polymer}} + (1 - w) \cdot H^{\text{clay}} \quad (4)$$

where  $w$  and  $(1-w)$  are the weight fractions of the polymer and the clay, respectively.

In Table 2, the additive values of the materials, calculated according to equation (4), are also included. The value of  $139 \pm 7$  MPa has been taken as microhardness of the neat clay [12].

The experimental microhardness values of the nanocomposites are plotted versus clay concentration in Fig. 5. The dashed line plots the corresponding additive values.

The results demonstrate (Table 2, Fig. 5) that the experimental microhardness values of the nanocomposites prepared by solution blending almost coincide with the corresponding additive values. On the contrary, the experimental microhardness values of the nanocomposites prepared by static annealing and melt blending are higher than the corresponding additive values. It should also be noted that the

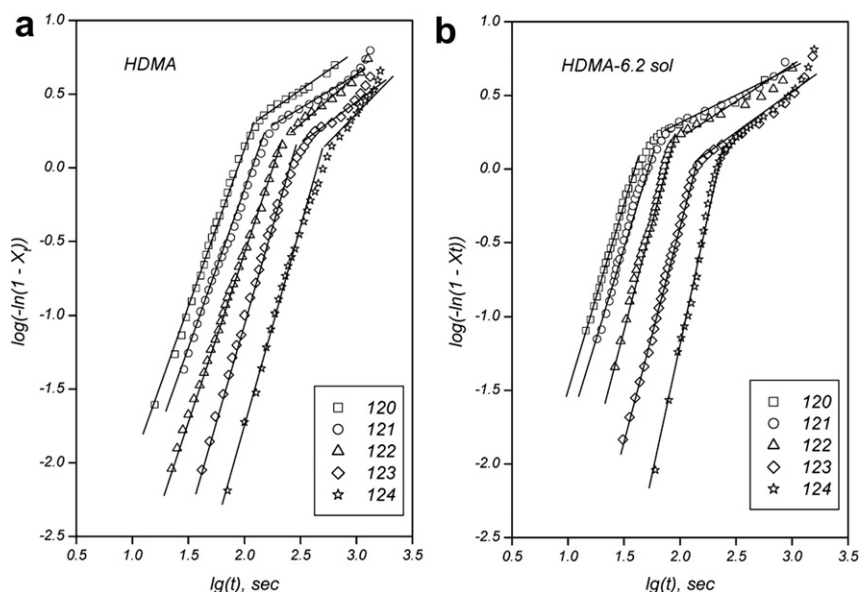


**Fig. 2.** Plots of  $\log(-\ln(1-Xt))$  vs.  $\log t$  for HDMA (a) and a nanocomposite, prepared by solution blending (HDMA-6.2 sol) (b).

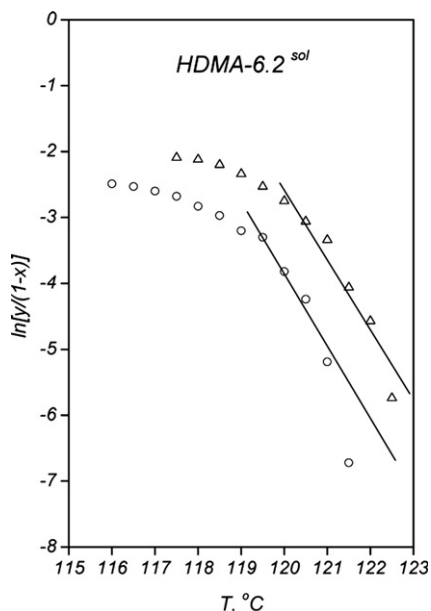


Fig. 4. Plots of  $\ln[y/(1-x)]$  vs.  $T$  for HDMA-6.2 composite, prepared by solution blending.

microhardness of melt blended samples is higher than that of samples prepared by annealing. These results could be interpreted by the different morphology of the materials obtained during the described procedures. It could be assumed that the good clay dispersion and high level of exfoliation achieved for nanocomposites prepared by melt blending and static annealing are the reason for the high values of the microhardness. It has been shown that poor filler dispersion and even filler agglomeration lead to lower microhardness values of functionalized polyethylene/clay [13] and compatibilized polyethylene/clay composites [14].

### 3.3. Measurements of limiting oxygen index (LOI) as a measure for the flammability of the nanocomposites

The limiting oxygen index has been determined by the volume ratio of the oxygen in the oxygen – nitrogen mixture at which the burned material still burns, i. e.:

Table 2

Experimental microhardness values ( $H_{exp}$ ) and additive microhardness values ( $H_{add}$ ) of the samples prepared by different procedures.

Sample	$H_{exp}$ , MPa	$H_{add}$ , MPa
HDMA	$61 \pm 3.0$	61
HDMA-6.2 (sol)	$65 \pm 3.0$	66
HDMA-10 (sol)	$70 \pm 3.5$	69
HDMA-15 (sol)	$74 \pm 3.7$	73
HDMA-25 (sol)	$79 \pm 4.0$	80
HDMA-6.2 (melt)	$75 \pm 3.7$	66
HDMA-10 (melt)	$80 \pm 4.0$	69
HDMA-15 (melt)	$84 \pm 4.2$	73
HDMA-25 (melt)	$86 \pm 4.3$	80
HDMA-6.2 (ann)	$72 \pm 3.6$	66
HDMA-10 (ann)	$74 \pm 3.7$	69
HDMA-15 (ann)	$79 \pm 4.0$	73
HDMA-25 (ann)	$84 \pm 4.2$	80

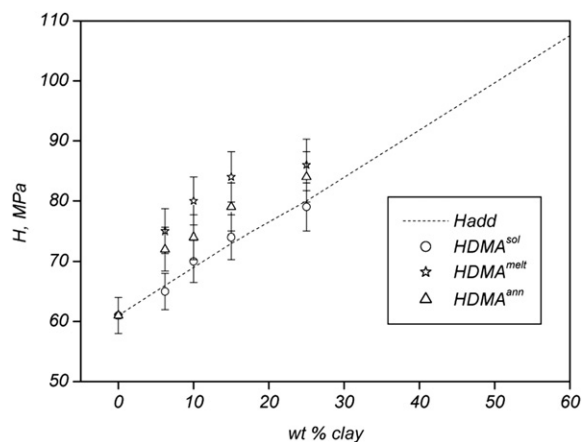


Fig. 5. Dependence of the microhardness on the clay concentration for HDMA composites, prepared by different procedures. The dash line represents the additive values.

$$LOI = O_2 / (O_2 + N_2)$$

The greater the LOI of a given material the lower is its flammability. The LOI values of the neat polymer and its nanocomposites, prepared by different procedures, are presented in Fig. 6. It is noteworthy that the neat polymer has a relatively high LOI. As seen, the nanocomposites have LOI higher than that of the neat polymer. That means the presence of the clay has reduced the flammability of the polymer. This reduction depends on the preparation procedure; the influence of clay for samples prepared by melt blending and annealing is more pronounced than that for the samples prepared by solution blending (Fig. 6). The reduction of the flammability is due to the accumulation of silicate on the surface of the burning specimen which creates a protective barrier to heat and mass transfer [12,15]. Evidently, the reasons for the stronger reduction of the HDMA flammability are the better dispersion and higher extent of exfoliation of the clay nanocomposites prepared by melt blending and annealing.

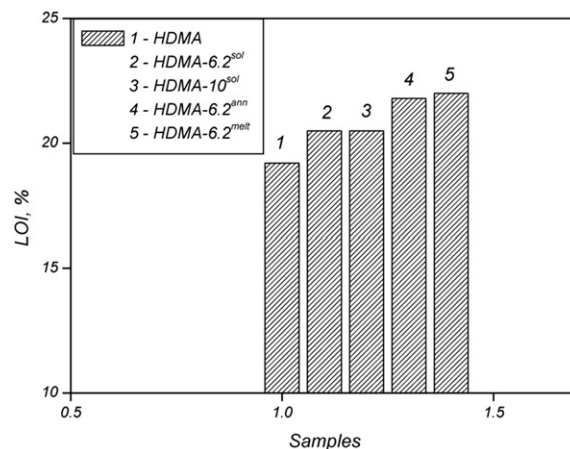


Fig. 6. Values of LOI of some samples.

#### 4. Conclusions

The study on the crystallization behavior, microhardness and flammability of HDMA nanocomposites, prepared by three different procedures, leads to the following conclusions: The reduction of the flammability and the increase in microhardness for HDMA/20A nanocomposites prepared by melt compounding and composite annealing are higher than those for composites prepared by solution blending. A nucleation effect of the clay on the polymer matrix crystallization for solution-blending samples has been observed. The results have been interpreted by different level of clay dispersion and degree of clay intercalation/exfoliation achieved during different preparation procedures. They reveal how the composite properties could be tailored to meet particular applications.

#### Acknowledgements

The research was supported by project of the National Science Fund (Project TK01/0110), Bulgaria. The authors

thank prof. P. L. Magagnini from the University of Pisa, Italy for the useful discussion.

#### References

- [1] L. Qiu, W. Chen, B. Qu, *Polymer* 47 (2006) 922.
- [2] F.C. Chiu, P.H. Chu, *J. Polym. Res.* 13 (2006) 73.
- [3] F.C. Chiu, S.M. Lai, J.W. Chen, P.H. Chu, *J. Polym. Sci. Part B* 42 (2004) 4139.
- [4] S. Hotta, D.R. Paul, *Polymer* 45 (2004) 7639.
- [5] S. Filippi, E. Mameli, C. Marazzato, P. Magagnini, *Eur. Polym. J.* 43 (2007) 1645.
- [6] S. Filippi, C. Marazzato, P. Magagnini, A. Famulari, P. Arosio, S.V. Meille, *Eur. Polym. J.* 44 (2008) 987.
- [7] M. Eder, A. Wlochowicz, *Polymer* 24 (1983) 1593.
- [8] K. Harnisch, H. Muschik, *Colloid Polym. Sci.* 261 (1983) 908.
- [9] F.J. Baltá Calleja, *Trends Polym. Sci.* 2 (1994) 419.
- [10] A. Flores, F.J. Baltá Calleja, D.C. Bassett, *J. Polym. Sci. B37* (1999) 3151.
- [11] J. Morawiec, A. Pawlak, M. Slouf, A. Galeski, E. Piorkowska, N. Krasnikowa, *Eur. Polym. J.* 41 (2005) 1115.
- [12] Y. Peneva, E. Tashev, L. Minkova, *Eur. Polym. J.* 42 (2006) 2228.
- [13] L. Minkova, Y. Peneva, M. Valcheva, S. Filippi, M. Pracella, I. Anguillesi, P. Magagnini, *Polym. Eng. Sci.* 50 (2010) 1306.
- [14] L. Minkova, Y. Peneva, E. Tashev, S. Filippi, M. Pracella, P. Magagnini, *Polym. Test.* 28 (2009) 528.
- [15] M. Zanetti, L. Costa, *Polymer* 45 (2004) 4367.